CHEMICAL ENGINEERING

Modeling and experimental evaluation of a non-isothermal photocatalytic solar reactor: temperature effect on the reaction rate kinetics

Modelado y evaluación experimental de un reactor solar fotocatalítico no isotérmico: efecto de la temperatura sobre la cinética de la velocidad de reacción

Molano M. Marena[1], Miguel A. Mueses[1], Machuca M. Fiderman[2§]

[1]Photocatalysis and Solar Photoreactors Engineering Department of Chemical Engineering, Universidad de Cartagena. Cartagena, Colombia.
[2]Gaox Research Group, Chemical Engineering School, Universidad del Valle. Cali, Colombia.
marena.molano@correounivalle.edu.co, mmueses@unicartagena.edu.co, fiderman.machuca@correounivalle.edu.co

(Recibido: Abril 26 de 2017 – Aceptado: Julio 09 de 2017)

Abastract

Mathematical modeling and experimental evaluation of temperature effects on photocatalytic degradation process and kinetic of a standard pollutants using solar radiation and suspended titanium dioxide were performed in a CPC reactor at pilot scale.

The model of the system includes mass balance of the batch reactor with recycle, based on global isotropic parameters. The incident radiation was modeled using empirical models adjusted using experimental data from environmental reports and optimization algorithms in function of atmospheric variations. The effect of scattering-absorption of radiation inside the reactor was estimated by solving the radiative transfer equation.

The effect of the temperature was modeled using a thermal balance coupled to heat transfer equations. The kinetic implemented model was a generalized model with a modification of the Arrhenius equation.

It was found that the temperature affected the reaction rates by varying the oxygen concentration during the reaction. Process performance was improved under normal operating conditions without temperature control. The mathematical model and the established solution algorithm were highly predictive, generating correlation coefficients of 0.99 and errors below 2.5%.

Keywords: *Thermal exchange, heterogeneous solar photocatalysis, LVRPA, Six-Flux Model, TiO2.*

Resumen

El modelado matemático y evaluación experimental de los efectos de la temperatura sobre la cinética de degradación fotocatalítica de una sustancia patrón utilizando radiación solar y dióxido de titanio suspendido fueron realizados en un reactor CPC a escala piloto acoplado a un intercambiador de calor para el control de la temperatura del sistema.

El modelo del sistema incluye el balance de masa del reactor discontinuo con reciclado, basado en parámetros isotrópicos globales. La radiación incidente se modeló utilizando modelos empíricos ajustados utilizando datos experimentales de informes ambientales y algoritmos de optimización en función de las variaciones atmosféricas. El efecto de dispersión-absorción de la radiación dentro del reactor se estimó mediante la resolución de la ecuación de transferencia radiativa.

El efecto de la temperatura se modeló usando un balance térmico acoplado a ecuaciones de transferencia de calor. El modelo cinético aplicado fue modificado con la ecuación de Arrhenius.

Se encontró que la temperatura afecta las velocidades de reacción por la variación de la concentración del oxígeno durante la reacción. El desempeño del proceso se mejora a condiciones normales de operación, sin control de temperatura. El modelo matemático y el algoritmo de solución establecidos son altamente predictivos, generando coeficientes de correlación de 0.99 y errores menores al 2.5%.

Palabras clave: *Intercambio térmico, fotocatálisis heterogénea solar, LVRPA, modelo de seis flujos, TiO2.*

1. Introduction

Heterogeneous photocatalysis is an advanced oxidation technology that consists of the absorption of radiant energy by a light-sensitive broadband semiconductor (1). The energy can be converted into heat or transferred to chemical bonds, resulting in electron/hole pairs that are transported and captured by species adsorbed onto the semiconductor surface. This process in turn leads to charge recombination and the formation of hydroxyl radicals, species responsible for degrading contaminant molecules through oxidation-reduction reactions (2). Heterogeneous photocatalysis has been implemented in removing a variety of organic compounds, recalcitrant liquids, and gaseous substances, especially: pesticides, herbicides, pharmaceuticals, inks, and others (3-5).

Because of its complex nature, fundamental research has been focused on laboratory scale, using artificial radiation with UV lamps in differential photocatalytic reactors under strict operating conditions (6), with low thermal energy dissipation by the fluid and the lamps. It has been observed that the temperature is not considered as a variable influencing the reaction rate, and therefore, these systems are assumed to be isothermal (7, 8).

However, the effects of heating on the operating conditions and using large-scale solar radiation leads to significant increases in temperature in radiation collection systems, which is the case with CPC reactors. These increases are based on environmental conditions and the amount of incident radiation, in addition to the fluctuations that may occur in the flow of energy from the sun. Some mathematical models have addressed the effects of energy emission corrected with cloudiness factors, the specific month of experimentation and the amount of total global incident radiation (9-11); however, the effects of increased temperature have not been considered in mathematical models of the kinetic law and reaction rate expressions.

This paper presents the experimental evaluation and mathematical modeling of the kinetic behavior of a heterogeneous photocatalytic degradation reaction of a standard substance in a solar CPC reactor at pilot scale by modifying a proposed model based on the Langmuir-Hinshelwood mechanism. Thus, the reaction fluid undergoes changes in temperature due to temporary energy fluxes caused by atmospheric fluctuations in electromagnetic light (12, 13). The rate constant is determined by the equation proposed by Arrhenius (14), and the adsorption constant is a variational parameter averaged over the temperature range of operation whereas a directly proportional relationship with the photonics component is kept via the effective quantum yield (10).

Methylene Blue (MB), is widely used in textile industry, is a common water pollutant and it is used as a standard compound due to its ability to accept or donate hydrogen ions in photocatalytic degradation studies (15), testing of photoreactors (16), and optimization of solar operations (17).

2. Methodology

2.1 Materials and equipment

For experimental evaluation, the following materials were considered: commercial grade Methylene Blue (MB), TiO_2-P25 Degussa (Evonik 99.8%) with a specific surface area of m^2/g, HCl (Panreac, 37%), and NaOH (Panreac, 2M). The experiments were carried out in a solar CPC reactor located at the University of Cartagena, Colombia (10°25'32"N 75° 32'59"W) coupled with a heat exchanger for regulating the temperature of the reaction fluid. The design parameters and equipment set-up are shown in Figure 1.

HEAT EXCHANGER SPECIFICATION SHEET		
Type: Double tube		
Connected in: Crosscurrent		
Length	1 m	
Fluid location	Annulus	Inner tube
Construction material	Galvanized iron	Copper
Nominal size (m)	0.076	0.019
Certificate / Type	20	Type K
Diameter (m) Internal / External	0.0856	0.019
Fluid Name	Water	200 ppm of MB
Temperature (°C) in/out	7 / 50	60 / 30
Caloric temperature (°C)	23.5	45
Dynamic viscosity (kg/m s)	9.22 10^{-4}	5.95
Specific heat (J/kg °C)	4.178	530.467
Fouling factor, Rd	0.001	
Total corrected coefficient design	53444.716	
ΔP (kg/cm^2)	0.492	
Total clean coefficient, Uc	621.199	
Total coefficient design, Ud	383.172	
Material	Commercial polystyrene black colored Absorptivity	
Thickness	10 mm	

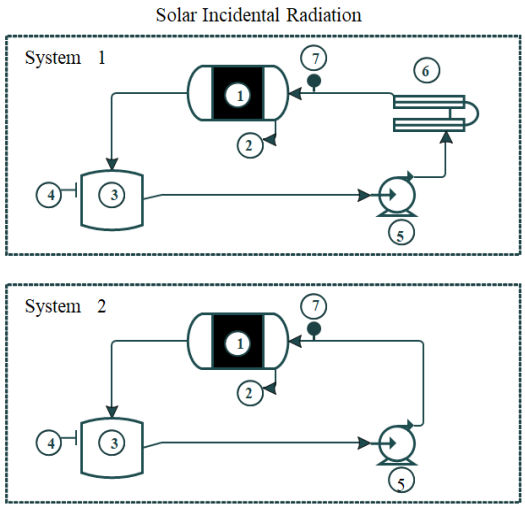

CPC SOLAR REACTOR	
Reactor material	Duran glass (1 tube)
Wall thickness (m)	0.014
Diameter (m)	0.032
Length (m)	0.834
Reaction volume (m^3)	0.004
Total volume of liquid	Without exchanger, 0.005 m^3 Exchanger, 0.015 m^3
Involute angle of reflection	90° 0.96
Transmittance	0.86

Figure 1. *Data Sheet for heat exchanger, reactor systems and study where: 1) CPC reactor, 2) involute, 3) tank, 4) sampling, 5) recirculating pump, 6) heat exchanger, and 7) thermocouple viewfinder.*

For this reactor, it was assumed perfect mixing and removal percentages of MB (%Degr) as response variable (19):

$$\%Degr = \left|\frac{C_0 - C_f}{C_0}\right| \times 100 \quad (1)$$

The fraction degraded is estimated according to the following equation:

$$C_{MB} = \frac{C}{C_0} \quad (2)$$

Here, C_0 is the initial concentration of the substrate, C is the concentration of the substrate for each experimental sample, and C_f is the final concentration of the substrate when the cumulative energy is 8000 J/m^2. The initial quantum yield is given in Equation 3.

$$\Phi_\lambda^0\big|_T = \frac{[R_i(x,t)^{t\to 0}]_{exp}}{\left[E_g^{\wedge a}{}_{(\lambda\to\lambda'),0}\right]_{Cal}} \quad (3)$$

where, $R_i(x,t)$ and $E_g^{\wedge a}{}_{(\lambda\to\lambda'),0}$ are the experimental reaction rate and the local volumetric rate of photon absorption, respectively. The applications of solar photocatalytic processes do not consider a uniform radiation field. Therefore, the intensive

character of the results is obtained by dividing by the volume of the reactor.

2.2 Experimental evaluation of the effect of temperature

For studying the photocatalytic degradation of MB, molecular absorption tests and four sets of experiments were carried out, as illustrated in Table 1. Two preliminary photolysis tests were carried out under non-preheated, isothermal reaction conditions to confirm that the possible thermal and photolytic reactions are not appreciable. To that end, a general procedure was developed for a photocatalytic test in the absence of a catalyst.

Table 1. *Experimental Methodology.*

Process	Condition reactor	Initial temperature (K)
Photolysis	Non-preheated	305
	Isothermal	312
Photocatalysis	Non-preheated	306
		305
	Preheated	323
		321
	Isothermal	307
		318

2.3 General procedure

Once the equipment was cleaned, systems 1 and 2 (see Figure. 1) were fed with 4 and 15 liters of water, respectively. Independet tests were performed for selection of better amount of catalyst; to this, 0.35 g/L of catalyst (Degussa P-25 TiO_2) was added at a low temperature and allowed to recirculate in the absence of light to ensure full mixing and adsorption equilibrium. Tests were performed base in a reaction mixture consisting in 200 mg/L of MB dissolved in natural water, at the pH of this mixture (6.95). Subsequently, the solution was subjected to solar radiation. For decolourization measurements, 10mL of sample was collected at 1000 J/m^2 of cumulative energy intervals until reaching a cumulative energy of 8000 J/m^2, temperature and adsorbance at 561 nm was measured.

Based on the temperature changes, different tests were carried out adjusting the water temperature in the reaction vessel to the initial temperature using the heat exchanger as shown in Table 1. Once the desired temperature was reacched, the general procedure continued as described above. Significantly, the photocatalytic processes are dependent on atmospheric changes, and therefore, it was very important to connect a heat exchanger to maintain a constant temperature for the reaction fluid entering into the reactor during the treatment period.

3. Reactor model

Mathematical modeling and simulation of photocatalytic reactors requires the use of several sub-models to describe the process successfully, including the emission model, the absorption model, the model of global effective quantum yield, and the fluid model dynamic. The reactor mass balance requires a kinetic model that satisfactorily represents substrate oxidation.

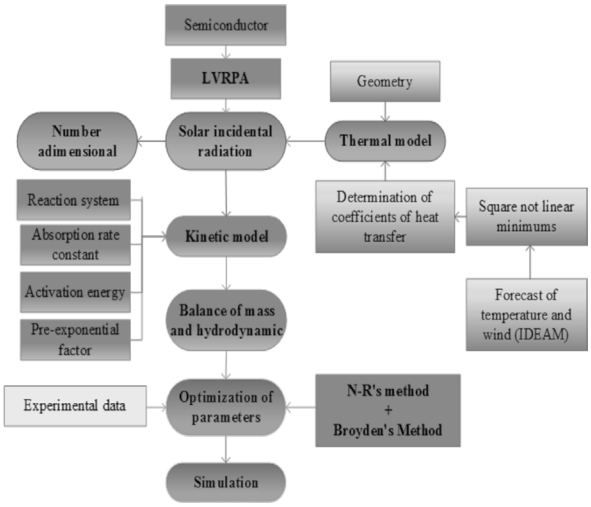

Figure 2. *Structure of the methodological model of a non-isothermal reactor.*

An expression of the reaction rate has been proposed by deriving it from the analysis of the reaction mechanism proposed by Turchi and Ollis (2), which considers that the molecular absorption of water and hydroxyl ions is the controlling step for the generation of hydroxyl radicals from the attack of the photo-generated holes. Then, the

volumetric rate of absorption of radiant energy serves as a correction factor for the effects associated with geometry, operating conditions and process scale. The mathematical methodology adopted by the authors is presented in Figure. 2.

3.1 Mass balance

Mass balance in the illuminated zone: The mass balance in the reactor coupled to the mathematical expression for the reaction rate referring only to the limiting reagent *i* and the reaction rate is given by Equation (4) and (5) (10):

$$r_i = -K_{Kin}\sqrt{E_g^{\wedge a}{}_{(\lambda\rightarrow\lambda')}}\frac{K_0 c_i}{1+K_0 c_{i,0}} \quad (4)$$

$$\frac{dC_i(t)}{dt} = \left(\frac{V_r}{V_t}\right)\kappa K_{Kin}\sqrt{E_g^{\wedge a}{}_{(\lambda\rightarrow\lambda')}}\frac{K_0 c_i}{1+K_0 c_{i,0}} \quad (5)$$

The progress of the photocatalytic reaction is affected naturally by the solar radiation, causing two main effects: cooling (when the light is reflected) and heating (when the light is absorbed). Therefore, the correction of the reaction rate is proposed through a function that evaluates the energy of the absorbed radiation per unit chemical energy of the wind:

$$\kappa = \left(\frac{Q_{Abs}\left(t\rightarrow t'\right)\times 100}{\dot{m}C_P T_a\left(t\rightarrow t'\right)}\right) \quad (6)$$

where $\lambda\rightarrow\lambda'$ y $t\rightarrow t'$ is the heat adsorbed in the reactor by the solar radiation. is the mass flow rate, C_p the specific heat capacity of the solution and T_a the air temperature, all of this are in the intervals $\lambda\rightarrow\lambda'$ y $t\rightarrow t'$ correspond to the absorption spectrum of the photocatalyst and to the treatment time, respectively.

3.2 Kinetics equation modified with temperature

The calculation of the kinetic constant K_{Kin} is performed by using the Arrhenius equation, which relates the changes in temperature via a pre-exponential factor K_a , the activation energy E_a, and the adsorption constant K_0 which is considered a variational parameter averaged over the temperature range of the process:

$$K_{Kin} = K_a e^{-E_a/T} \quad (7)$$

$$K_0 = \frac{1}{\Delta T}\int K dT \quad (8)$$

where, K_{Kin} is the reaction rate kinetic constant (mol/m^{2}s), C_i is the substrate concentration (mol/m^3), $E_g^{\wedge a}$ is the global volumetric rate of photon absorption (Einstein/m^{3}s), and K_0 is the Langmuir-Hinshelwood kinetic constant (m^3/mol).

Mass balance in the dark zone: The reactor outlet concentration for each step is coupled with the inlet concentration that comes from the piping system and the storage tank, known as the recycling zone (10). The mass balance in this area is

$$C_{i,\tau_{pass+1}} = \frac{C_{i(\tau_{pass})}[V_t - V_r] + C_{i(\tau_{pass})}V_r}{V_t} \quad (9)$$

The proposed model was incorporated into the mass balance, which is expressed as an equation by reaction step at steady state evaluated at each residence time τ_{pass} . In this way, the batch reactor is described as a finite sum of steps $N_{pass,Total}$ (10) .

$$N_{pass,Total} = \frac{t_{total,Q_{acu,Total}}}{\tau_{pass}} \quad (10)$$

Typically, the interpretation of the experimental results is based on t_{30w} (19), the treatment time (20), the incident radiation within the reactor, and the photon flux absorbed by the catalyst. However, these parameters interact and yield erroneous conclusions, which is impractical given that the reactor is comprised of illuminated and non-illuminated areas.

For being consistent with the analysis of the results resulting from the use of two different systems, the temporal distribution of solar radiation incident on the earth's surface (21) is used to represent the evolution of the photocatalytic process according to the energy

accumulated by the reactor over time as well as to compare the efficiency of different intrinsic photoreactors by the following equation:

$$\frac{dC_i}{dt} = \frac{dC_i}{dQ_{acu}} \cdot \frac{dQ_{acu}}{dt} \qquad (11)$$

The UV/vis irradiation was measured using a digital radiometer HD 2102.2, and was used to the evaluation of the change in the cumulative energy with respect to the treatment time , as illustrated in Figure 3 corresponding to the experimental test period considered in this work. To provide a reproducible conditions, all the experiments were carried out near noon, when the solar radiation was moderately stable.

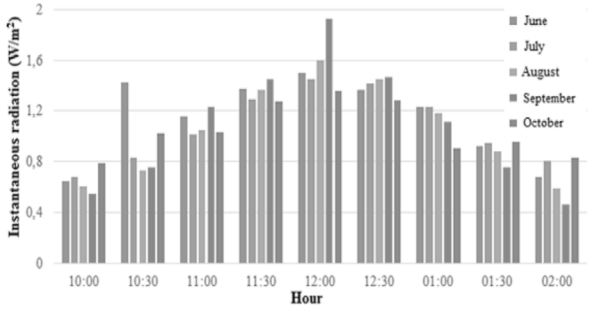

Figure 3. *Distribution of instantaneous radiation vs time.*

3.3 Thermal balance

Power variations in the reaction fluid are caused both by the energy absorbed through the reactor wall, the optical properties of which remain constant (as does the specific heat of the reaction fluid), and by system components. Thus, it is assumed that the fluid phase does not absorb radiation, the reactor wall does not allow the entry of radiation below 240 nm, and the catalyst does not absorb radiation above 380 nm. In addition, the temperature profile is uniform around the outer wall of the reactor (22, 23). Figure 4 shows the control volume of the CPC reactor.

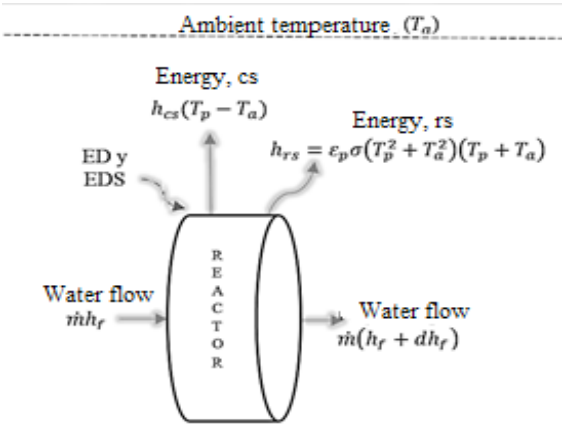

Figure 4. *Schematic of the energy balance in a differential section area of a CPC reactor.*

From this, the absorbed solar power is determined as shown below:

$$Q_{Abs} = IA_a\eta \qquad (12)$$

$$\eta = \tau\rho\alpha \qquad (13)$$

where τ,ρ and a are the transmittance, reflectance and absorptance of borosilicate glass. I is intensity of radiation and A_a is the transversal area of the reactor. In this paper, an empirical model of fitting functions that characterize the behavior of the mass flow of the wind V_a and the temperature T_a is implemented based on data provided by IDEAM in Colombia, (24) according to the following procedure.

Hourly averages were calculated from 9:00 a.m. until 2:00 p.m. for each month of the experimental test. The data obtained were fitted using non-linear least squares and are reported as their respective correlation coefficients. The main energy flows are described through the mechanisms of heat transfer as follows (25).

Radiation losses from the reactor wall to the environment.

$$Q_{rs} = h_{rs}(T_p - T_a) \qquad (14)$$

Losses from free or forced convection from the reactor wall to the environment.

$$Q_{cs} = h_{cs}(T_p - T_a) \qquad (15)$$

The coefficients of heat transfer by radiation and convection between the surface of the reactor wall and the environment are determined by the following equations:

$$h_{rs} = \varepsilon_p \sigma \left(T_p^2 - T_a^2\right) \quad (16)$$

$$h_{cs} = \frac{\dot{m} C_p \left(T_{(0,t)} - T_a\right)}{A_a \left(T_{(0,t-1)} - T_a\right)} \quad (17)$$

Where ε_p is the emissivity and σ is called the Stefan–Boltzmann constant. T_p is the average temperature between air and solution temperature. $T_{(0,t)}$ and $T_{(o,t\text{-}1)}$ and correspond to the temperatures of the reactor wall measured at the outlet and inlet of the reactor, respectively, obtained as an average between the reaction fluid temperature and the ambient temperature for each sampling point. Whereas, the overall energy equation is used to determine the heat added by the system due to pipe friction h_L, and the use of the centrifugal pump h_A, whereby it acquires the following form:

$$Q_{sis} = h_A - h_L \quad (18)$$

This system of equations takes the following form:

$$Q_{útil} = \dot{m} C_{P_{AM}} \left(T_{out} - T_{in}\right) = Q_{Abs} - \left(Q_{rs} + Q_{cs}\right) + Q_{sis} \quad (19)$$

3.4 Calculation of the LVRPA

For complete modeling of reactor, quantification of the volumetric rate of absorption of radiant energy, LVRPA, is performed using the SFM (19):

$$LVRPA = \frac{I_0}{\lambda_{corr} \omega_{corr} (1-\gamma)} \left[\left(\omega_{corr} - 1 + \sqrt{1 - \omega_{corr}^2} \right) e^{\frac{-\gamma}{\lambda_{corr}}} + \gamma \left(\omega_{corr} - 1 - \sqrt{1 - \omega_{corr}^2} \right) \right] \quad (20)$$

where I_0 is the intensity of radiation incident on the wall of the reactor equivalent to 30W/m^2, λ_{corr} is the extinction length, ω_{corr} is the scattering albedo coefficient, and γ is the point coordinate in the reaction space (19, 26, 27). These parameters were estimated through the methodology proposed by Colina-Márquez et al. using the optical properties of the catalyst and the solar radiation conditions in Cartagena, Colombia (28).

4. Results and discussion

Degradation processes under direct photolysis did not contribute to the process of photocatalytic degradation; in the non-preheated condition percentages of degradation of 11% and 9.5% for the isothermal condition at 312 K were obtained. In addition, photolysis can contribute with the degradation mechanism.

Because the phenomena of convection and radiation exert a cooling effect on the reaction fluid throughout the process to prevent any solar power from being exploited as useful heat, it is not possible to develop a study of the thermal behavior of the reactor in a deterministic method. As a result, the treatment of climatological data was performed via nonlinear least squares, thereby obtaining mathematical expressions describing the wind speed in m/s and its temperature (°C) as a function of the time of day during the experiment months with respect to the correlation coefficients as described below:

June

$$V_a = -0.2198t^2 + 5.7025t - 2.6441, R^2 = 0.9994 \quad (21)$$

$$T_a = 0.0517t^3 - 1.7351t^2 + 19.159t - 66.318, R^2 = 0.9851 \quad (22)$$

July

$$V_a = -0.2163t^2 + 5.5374t - 2.0067, R^2 = 0.9963 \quad (23)$$

$$T_a = 0.2062t^2 - 4.2826t + 24.024, R^2 = 0.9973 \quad (24)$$

August

$$V_a = -0.2675t^2 + 6.7388t - 9.0823, R^2 = 0.992 \quad (25)$$

$$T_a = -0.0169t^3 + 0.7279t^2 - 9.7893t + 44.147, R^2 = 0.9889 \quad (26)$$

September

$$V_a = -0.254t^2 + 6.429t - 7.0516, R^2 = 0.9982 \quad (27)$$

$$T_a = 0.0494t^3 - 1.5756t^2 + 16.344t - 52.379, R^2 = 0.9864 \quad (28)$$

October

$$V_a=-0.2703t^2+6.7131t-8.6796, R^2=0.9918 \quad (29)$$

$$T_a=0.043t^3-1.4322t^2+15.545t-53.118, R^2=0.9823 \quad (30)$$

By using the structure in Figure 2, it was found that the kinetic parameters K_a, E_a, and K_o were 2±0.1 mol/ms, -29.1±34 J/mol, and 1.9±0.1 m^3/mol, respectively. This equation yields a minimum R^2 of 0.938 and a maximum standard deviation of 0.178. Moreover, the energies that systems 1 and 2 added were 8.11 W and 6.11 W, respectively. The results demonstrated that cooling system is not recommended because the radiation causes only moderate increases in temperature that are beneficial to the process (Table 2). This means that the temperature could be important in the catalyst structure under normal operating conditions.

The predictive capacity of the model, associated with the use of a correction because of the effect of atmospheric variations over timeκ, is attractive for considering high substrate concentrations and temperature fluctuations (Figure 5). The calculated kinetic parameters can be used to evaluate the performance of the catalyst at higher temperatures, provided that a tubular or CPC reactor is used (29, 30). Similarly, the energy of absorbed radiation per unit chemical energy of wind κ can be used to evaluate the thermal performance of the reactor. Nevertheless, this is a first pass to interpret the process that appear during the reaction in atmospherics conditions because there is no literature report yet.

Table 2 summarizes the useful heat, the heat absorbed, the dimensionless number, the percentage of degradation, and the initial quantum yield obtained by evaluating the LVRPA at the reactor wall.

***Table 2**. Kinetic parameters adjustment for photocatalytic degradation AM.*

Condition	Initial T. (K)	$Q_{Abs}[W]$	$Q_{útil}[W]$	$100/\kappa$	%Degr.	$\ddot{O}^o_\lambda\big\|_T \left[\frac{mol}{einstein}\right]$
Photolysis	305	0.0365	5.0400	0.0998	11	---
Isothermal photolysis	312	0.0497	7.8124	0.1469	9.5	---
Non-preheated	304	0.0556	5.6107	0.6710	32.80	$2.2573\ 10^{-7}$
	305	0.0371	9.3752	0.0782	45.94	$1.1631\ 10^{-9}$
Preheated	323	0.0443	5.5694	0.3890	41.80	$1.9616\ 10^{-7}$
	321	0.0576	5.9326	0.5525	38.50	$2.4446\ 10^{-7}$
Isothermal	307	0.0615	8.0849	0.1861	13.48	$3.6472\ 10^{-7}$
	318	0.0838	7.6748	0.2479	33.21	$1.1336\ 10^{-6}$

For this study, we considered that the kinetic parameters found point out that the reaction proceeds in two stages. The first stage corresponds to adsorption and the second to the reaction. When the temperature is increased, the reaction stage is favored, increasing the number of effective collisions between molecules and disfavoring the adsorption stage because the equilibrium shifts to the formation of less substrate-semiconductor complex (18). However, the results can be described by first-order kinetics that is slightly favored when the temperature is increased (Figure 5).

For different conditions, the rate of photocatalytic reaction abandons its dependence on the intensity of solar radiation, temperature, and wind speed when the dimensionless parameter assumes values above 0.2, probably because the processes of mass transfer in the midst of the reaction.

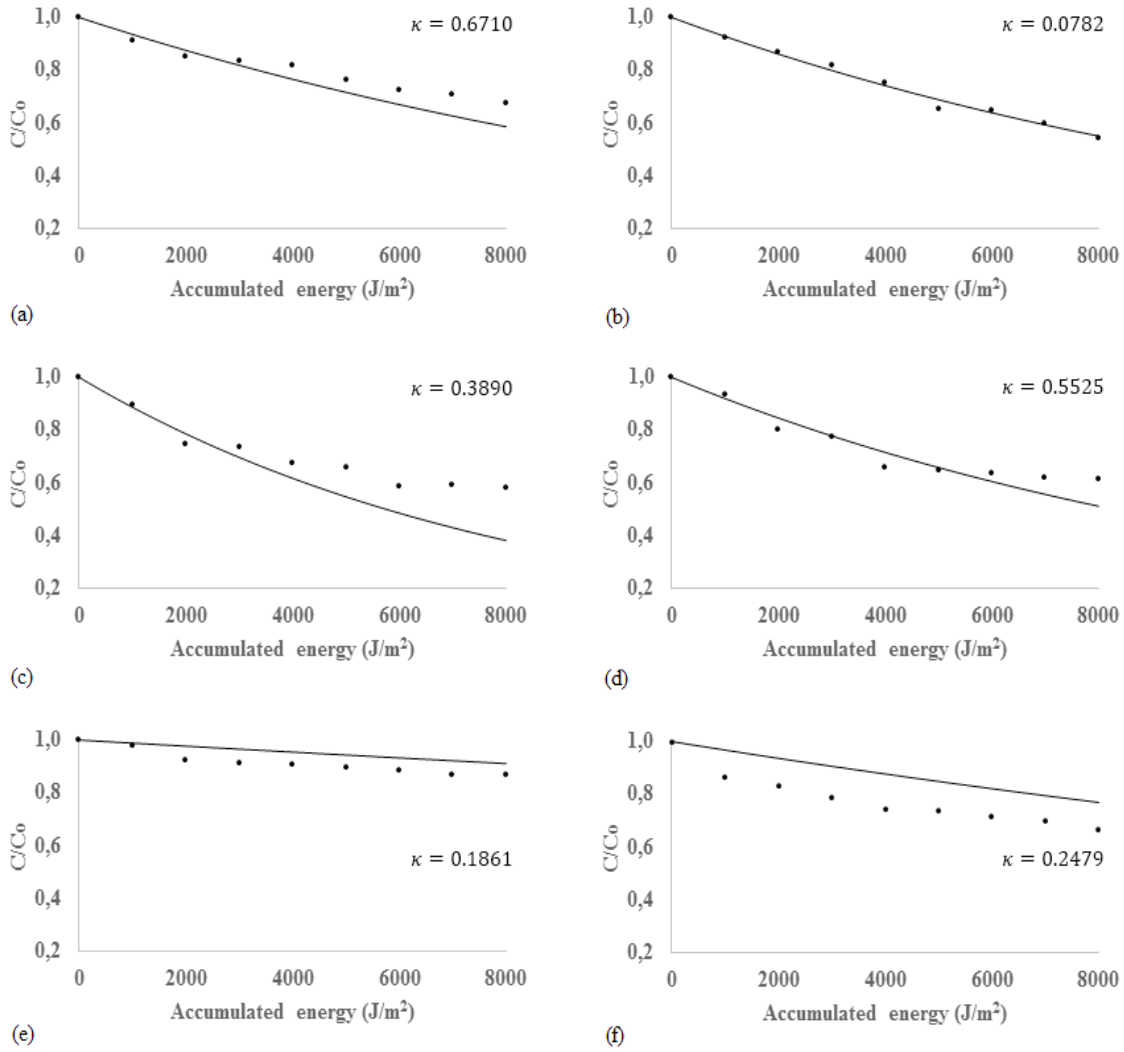

Figure 5. *Adjusting experimental kinetic data for the solar heterogeneous photocatalytic degradation CPC reactor: (a) not preheated to 306 K, (b) not preheated to 305 K, (c) preheated to 323 K, (d) preheated to 321 K, (e) isothermal at 307 K and (f) at isothermal at 318 K.. Experimental data (●), Reaction rate model (-). The model reaction rate includes the effect of temperature.*

5. Conclusions

A new model for the description of the heterogeneous photodegradation of Methylene Blue using TiO_2 was formulated from a mechanism based on the attack of hydroxyl radicals and considering the atmospheric changes that cause heating of the process fluid through a balance of matter and energy. The resulting model has a simple mathematical structure with a correction term for the effects of variation of the radiation intensity, temperature, and wind speed, i.e., as a function of weather and reaction geometry.

For the non-preheated reactor condition, the model adequately describes the processes of charge transfer, unlike the preheated and isothermal reactor conditions. The kinetic parameters obtained from this model are associated strictly with the radiant field configuration and the nature of the substrate. Consequently, the proposed model can be generalized and used in the treatment of organic

pollutants by heterogeneous solar photocatalysis. In addition, since our experiments, a detailed reaction mechanism could be presented considering the electronic properties of the catalyst.

The experimental evaluation shown that the temperature effects over the system affected the performance, when the temperature is increased the reaction stage is favored, the first-order kinetics that is slightly favored too and disfavoring the adsorption stage.

6. References

(1) Ballari, M. d, Brandi, R., Alfano, O, Cassano, A. Mass transfer limitations in photocatalytic reactors employing titanium dioxide suspensions: 1. Concentration profiles in the bulk. Science Direct, 136 (2008) 50-65.

(2) Turchi, C. S., Ollis, D. F. Photocatalytic Degradation of Organic Water Contaminants: Mechanisms Involving Hydroxyl Radical Attack. Journal of Catalysis, 122 (1990) 178-192.

(3) Garza-Campos, B, Brillas, E., Hernández-Ramírez, A, Ghenymy, A, Guzmán-Mar, J. L, Ruiz-Ruiz, E. J. Salicylic acid degradation by advanced oxidation processes. Coupling of solar photoelectro-Fenton and solar heterogeneous photocatalysis. Journal of Hazardous Materials, 319 (2016) 34-42.

(4) Carabajo, J, Jiménez, M., Miralles, S, Malato, S, Faraldos, M, Bahamonde, A. Study of application of titania catalysts on solar photocatalysis: Influence of type of pollutants and water matrices. Chemical Engineering Journal, 291 (2016) 64-73.

(5) Bayarri, B, Giménez, J, Maldonado, M. I, Malato, S, Esplugas, S. 2,4-Dichlorophenol degradation by meanso of heterogeneous photocatalysis. Comparison between laboratory and pilot plant performance. Chemical Engineering Journal, 232 (2013) 405-417.

(6) Carneiro, J. T, Moulijn, J. A, Mul, G. Photocatalytic oxidation of cyclohexane by titanium dioxide: Catalyst deactivation and regeneration. Journal of Catalysis, 273 (2010) 199-210.

(7) Alfano, O. A, Bahnemann, D, Cassano, A. E, Dillert, R, Goslich, R. Photocatalysis in water environments using artificial and solar light. Catalysis Today, 58 (2000) 199-230.

(8) Zalazar, C. S, Labas, M. D, Marín, C. A, Brandi, R. J, Alfano, O. M., Cassano, A. E. The extended use of actinometry in the interpretation of photochemical reaction engineering data. Chemical Engineering Journal, 109 (2005) 67-81.

(9) Colina-Márquez, J, Machuca-Martínez, F, Li Puma, G. Modeling the Photocatalytic Mineralization in Water of Commercial Formulation of Estrogens 17-β Estradiol (E2) and Nomegestrol Acetate in Contraceptive Pills in a Solar Powered Compound Parabolic Collector. Molecules, 20 (2015) 13354-13373.

(10) Mueses, M. A, Machuca-Martinez, F, Li Puma, G. Effective quantum yield and reaction rate model for evaluation of photocatalytic degradation of water contaminants in heterogeneous pilot-scale solar photoreactors. Chemical Engineering Journal, 215-216 (2013) 937-947.

(11) Colina-Márquez, J, López-Vásquez, A., Díaz, D, Rendón, A, Machuca-Martínez, F. Photocatalytic treatment of a dye polluted industrial effluent with a solar pilot-scale CPC reactor. Journal of Advanced Oxidation Technologies, 12 (2009) 93-99.

(12) Jaramillo Páez, C. A., Taborda Ocampo, G. La Fotocatálisis: Aspectos fundamentales para una buena remoción de contaminantes. Revista Universidad de Caldas, 26 (2006) 71-88.

(13) Machuca-Martínez, F. Cálculo de parámetros cinéticos en reacciones fotocatalíticas usando un modelo efectivo de campo de radiación. Ingeniería y Competitividad, 13 (2011) 25-40.

(14) Barka, N., Qourzal, S., Assabbane, A., Nounah, A., Ait-Ichou, Y. Photocatalytic Degradation of an Azo Reactive Dye, Reactive Yellow 84, in Water Using an Industrial Titanium Dioxide Coated Media. Arabian Journal of Chemistry, 3 (2010) 279-283.

(15) Baquero Dulceyr, M. I, Sterling López, A. M, Mera Benavides, C. Biological-photo catalytic combination for the treatment of complexometric waste materials generated in chemical and environmental analysis laboratories. Revista Lasallista de Investigación, 7 (2010) 7-16.

(16) Khadijeh Beigom Ghoreishi, Nilofar Asim, Zatil Amali Che Ramli, Zeynab Emdadi, M. Ambar Yarmo. Highly efficient photocatalytic degradation of methylene blue using carbonaceous WO_3/TiO_2 composites. Journal of Porous Materials, 23 (2016) 629-637.

(17) Galagan, Y, Su, W.-F. Reversible photoreduction of methylene blue in acrylate media containing benzyl dimethyl ketal. Journal of Photochemistry and Photobiology, 195 (2008) 378-383.

(18) Rodríguez-Acosta, J. W, Mueses, M. A, Machuca-Martínez, F. Mixing Rules Formulation For a Kinetic Model of the Langmuir-Hinshelwood Semipredictive Type Applied to the Heterogeneous Photocatalytic Degradation of Multicomponent Mixtures. International Journal of Photoenergy, 2014 (2014) 0-9.

(19) Colina-Márquez, J. A, Machuca-Martínez, F, Li Puma, G. (2010). Radiation absorption and optimization of solar photocatalytic reactors for environmental applications. Environmental Science Technology, 13 (2010) 5112-5120.

(20) Grčić, I., Li Puma, G. Photocatalytic Degradation of Water Contaminants in Multiple Photoreactors and Evaluation of Reaction Kinetic Constants Independent of Photon Absortion, Irradiance, Reactor Geometry and Hydrodynamics. Environmental Science & Technology, 47 (2013) 13702-13711.

(21) Rodriguez M, H, Gonzales B, F. Manual de radiación solar en Colombia. Bogotá: Gonzales y Rodriguez. (1994).

(22) Zalazar, C. S, Satuf, M. L, Cassano, A. E. Comparison of H_2O_2/UV and Heterogeneous Photocatalytic Processes for the Degradation of Dichloroacetic Acid In Water. Enviroment Science Technology, 42 (2008) 6198-6204.

(23) Lukaski, A, Muggli, D. Photocatalytic oxidation of dichloroacetic acid and dichloroacetyl chloride on TiO_2: active sites, effect of H2O, and reaction pathways. Catalysis Letter, 89 (2003) 129-138.

(24) IDEAM (Colombia). IDEAM - Subdirección de Meteorología Grupo De Modelamiento De Tiempo Y Clima. (2015) Retrieved from http://bart.ideam.gov.co/wrfideam/colombia/SKCG.txt

(25) Kern, D. Q. Process Heat Transfer. México: Compañía Editorial Continental S.A. de C.V. (1965).

(26) Li Puma, G, Brucato, A. Dimensionless analysis of slurry photocatalytic reactors using a two-flux and six-flux radiation absorption-scattering models. Catalysis Today, 122 (2007) 78-90.

(27) Mueses, M, Colina-Márquez, J, Machuca Martínez, F. Degradación fotocatalítica de ácido dicloroacético al aplicar un campo de radiación de baja energía. Ingeniería y Desarrollo. Universidad del Norte, 24 (2008) 33-47.

(28) IDEAM (Colombia). Atlas de Radiación Solar, Ultravioleta y Ozono de Colombia. (2015) Retrieved from http://atlas.ideam.gov.co/visorAtlasRadiacion.html

(29) Klamerth, N, Miranda, N, Malato, S. Degradation of emerging contaminants at

low concentrations in MWTPs effluents with mild solar photo-Fenton and TiO_2. Catalysis Today, 144 (2010) 39-45.

(30) Zhong, J, Liu, Z, Shi, J, Zhang, Y, Hu, H, Shangguan, W. Degradation of indoor gaseous formaldehyde by hybrid VUV and TiO2/UV processes. Separation and Purification Technology, 54 (2007) 204-211.